Egyptian Journal of Chemistry

http://ejchem.journals.ekb.eg/

Structural and Biological Features of Cu, Mg Co-Doped Hydroxyapatite Prepared by Wet Chemical Precipitation

Aala S. Najim [1*], Firas J. Hmood [1], Israa K. Sabree [1]

1 Department of Ceramics and Building Materials/ College of Materials Engineering/ University of Babylon ,Najaf-hilla St. , 51001, Babylon, Iraq

Abstract

The pure hydroxyapatite (HAp) and antibacterial co-doped hydroxyapatite [(Cu, Mg) HAp] nano-powders were synthesized by Wet chemical precipitation method. Calcium hydroxide ($CaOH_2$) and phosphate acid (H_3PO_4) were utilized as starting materials, magnesium oxide (MgO) and copper oxide (CuO) represent the doping elements . The ratio (Ca/P) kept at 1.67 and PH value maintained to10 at room temperature. Pure HAp [$Ca_{10}(PO_4)_6OH_2$] and three stoichiometric compositions of the co-doped HAp were prepared which were [$(Mg_{0.25},Cu_{0.75})Ca_9(PO_4)_6OH_2$],[$(Mg_{0.5},Cu_{0.5})Ca_9(PO_4)_6OH_2$] and [$(Mg_{0.75},Cu_{0.25})Ca_9(PO_4)_6OH_2$]. All the prepared powders were calcinated at 800 °C for 2hrs . The structure, antibacterial activity, and toxicity with cell viability have been investigated using several characterization techniques . XRD results showed that the fabricated undoped- HAp and co-doped HAp has one (hexagonal) phase , and the FT-IR results shows functional group that confirm the results of XRD. The TEM images indicated that incorporation of Cu^{2+} and Mg^{2+} has altered the size and morphology of the resulting HAp crystals which appears elongated with dissimilar sizes. Antibacterial test indicated that co-doped HAp [$(Mg_{0.25},Cu_{0.75})Ca_9(PO_4)_6OH_2$] showed high activity versus E.coli and S.aureus bacteria. The MTT assay for the [$(Mg_{0.75},Cu_{0.25})Ca_9(PO_4)_6OH_2$] has shown superior positive role on cell viability as appears in the fluorescent image, and has acceptable antibacterial activity.

Keywords: co-doped hydroxyapatite; wet chemical precipitation; nano powder; antibacterial activity; cytotoxicity; Bioceramic; bone repair

1. Introduction

The calcium phosphates (CaP) compounds are materials that Significantly utilized in biomedical applications. The bone formation is predominantly contains calcium phosphates as hydroxyapatite [$Ca_{10}(PO_4)_6(OH)_2$] , corresponding to a ratio between 65% and 70% of the bone structure [1]. Among the wide mole ratios of calcium phosphates, 1.67 is considered the most attractive one which belongs to hydroxyapatite $Ca_{10}(PO_4)_6(OH)_2$, and is highly used in the clinical applications such as orthopaedic implants and restorative dental [2, 3]. In addition, it has excellent bio affinity and has role in Osseo- integration enhancement [3]. The structure of hydroxyapatite consists of calcium ions and phosphate groups in addition to hydroxyl groups. All of them are assembled in hexagonal unit cell [4]. This structure has the ability to accommodate ions substitutions (one [5], two [6], three [7] cations or anions) of various ions (e.g. Sm^{3+}, F^-, Cl^- , Na^+, K^+, Mg^{2+}, K^+, Sr^{2+}, $Ba.^{2+}$, Al^{3+}, Mn^{2+}, Cu^{2+}, Al^{3+}, Zn^{2+}, Ag^+, Ce^{3+}, Eu^{3+},) [8]. The substitution is based on the charge of the HA ions; i.e. Mg^{2+}, Mn^{2+}, or Sr^{2+} are hosted by the locations of calcium cations. Conversely the SiO_4^{4-} and

BO_3^{3-} ions picked the locations of phosphate ions, the hydroxyl ions locations might occupied by other ions in the same size and charge i.e. (CO^-, Cl^- or F^-) [9, 10,11]. In this ions exchange the deference in sizes and charges of ions causes alteration in the dimensions of the HAp unit cell. Those substitutions are necessary to develop the biological, mechanical and physic-chemical properties of HAp. The wet chemical precipitation is widely used to synthesize doped hydroxyapatite among many methods. Because this method ensures ultrahigh purity, simplicity, as well as nanoparticle size. The parameters that control this method are starting materials, pH of the precursors, precipitation temperature, and mixing speed [12]. All these parameters can affect the properties of the resulting HA powder. One of HAp drawbacks is lack of antibacterial properties. Limitation of antibacterial resistance and bacterial infections are the main causes of implant failure [13]. In orthopedics , the plurality of infections after surgeries are related with the existence of implants[14]. In the literature, it has been stated that consolidation of Ag, Cu and Zn ions into

the implants is important to prevent or minimize the bacterial adherence in the initial state [15]. Yan Li et al investigated the antibacterial and cytotoxicity features of Cu^{2+} and Ti^{4+} doped hydroxyapatite prepared by wet chemical method. The Cu^{2+} doped hydroxyapatite appeared good antibacterial resistance versus Escherichia coli. This may be happened due to leaching of copper ions (Cu^{+2})which leads to cause lysis of bacteria, but the existence of copper ions remain cytotoxic to osteoblasts.
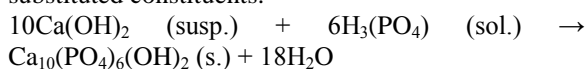
The doped Ti-HAp presented antibacterial properties when the Ti molar ration is high, with a slight toxicity to osteoblasts [16]. Another study dealt with incorporation of Zn-and Mg- together into chemically precipitated HAp. It showed that the antibacterial effect on Gram(+) and Gram(-) bacteria was better than the single doping of each element into HAp [17]. Similarly, incorporation of strontium and cerium into HAp (Sr, Ce)-HAp exhibited good inhibition for the E. coli and S.aureus bacteria [18].

The goal of this research is to investigate the effect of mole ratio variation of double metal (Cu^{2+} and Mg^{2+}) ions that partially replaced by Ca^{2+} cations on the structural and biological features of hydroxyapatite.

2. Experimental work
2. 2.1 Starting materials and sample preparation
The materials that used in wet chemical precipitation method were H_3PO_4 (85 wt%) (Thomas Baker, India) with a purity > 98 %, $Ca(OH)_2$ has a of purity > 98% (Fluka AG, Germany), MgO and CuO (both have purity > 99%) (Sigma Alrditch, Germany). The concentrations of all the reagents were calculated considering the molar ratio of (Ca/P = 1.67) of HA. The mole ratio of the co-doped HA was kept to ((Mg+Cu+Ca)/P) 1.67 as well. The full ions substitution was (1(Cu+Mg) / 9Ca). Three mole ratios of Cu^{2+} and Mg^{2+} were chosen i.e. 0.25:0.75, 0.5:0.5, and 0.75:0.25. The following chemical reaction was employed to calculate the mole ratios of the substituted constituents:

$10Ca(OH)_2$ (susp.) + $6H_3(PO_4)$ (sol.) → $Ca_{10}(PO_4)_6(OH)_2$ (s.) + $18H_2O$

$Ca(OH)_2$ 0.1 M was prepared by mixing $Ca(OH)_2$ with water using an overhead stirrer at 20°C. Then diluted solution of H_3PO_4 (0.06 M) was added drop-wise (1.5 ml / min) to the slurry with continuous stirring (800 rpm) at room temperature. The solution PH was kept at 10. The reactants were continuously stirred (400 rpm) for further 24 h at room temperature. For the preparation of co-doped HA, the required amounts of CuO and MgO were dissolved in H_3PO_4 by stirring (400 rpm) for about 1 h, then the same preceding method has been conducted to prepare (Cu, Mg) HA. After aging process end, the precipitated compound were filtered and the

deionized water used to wash for times after that dried at 110 ◦C. Table 1 shows the reactant materials that utilized in this method

2.2 Characterizations
2.2.1 Thermal analysis
The thermal analysis was done using a thermo gravimetric analysis (TGA) equipped with differential thermal analysis (DTA) (TA-Q600.USA). The samples were non-isothermal heated. The test was done in atmosphere condition with heating rate of 10 $^{\circ}$C/ min and up to 850°C.

2.2.2 Phase identification
X-ray diffraction (XRD) method was utilized to identify the resulting phases of the synthesized HAp. An XRD machine (Shimatzu 6000 diffract meter, Japan) was used for this purpose. The Nickel was utilized as filter ,and Copper-kα was utilized as a radiation source with 40 kV and 30 mA and 5°/min as a scan speed. The diffraction data were recorded in the range of 2θ = 20 - 60° with a scanning speed of 0.05°.

The degree of crystallinity (X_c) (degree of structure order) was calculated for undoped and doped HAp in the following equation:

$$X_c \approx 1 - \frac{V112/300}{I_{300}}............[25]$$

where I 300 is related to the intensity plane (300) while V 112/300 is related to the intensity of the space reflections between plane(112) and plane(300) [25]. The structural groups of the HAs were specified using a Fourier transformation infrared spectrophotometer FTIR (Shimatzu 1800, Japan) over the range from 3600 to 400 cm^{-1} at 4 cm^{-1}

2.2.3   Shape of particles
The shape of particles of synthesized HAp and co-doped HAp powders was observed using a transmission electron microscope (TEM) (Philips CM120).

2.2.4 Biological Tests
2.2.4.1 Antimicrobial activity test
The antibacterial activity of the synthesized HAp was determined by the standard agar well diffusion method versus two bacterial strains E. coli (ATCC 25922) and S. aureus (ATCC 25923). The diffusion test for agar was done at Müller-Hinton agar. The agar was poured into petri discs in order to form a layer with thickness of 4mm, after that the inoculation for the dense micro-organisms has been done to acquire semi-confluent growth. The solution with a constant concentration of (250 µg/ml) was

_____

prepared by dissolving the undoped and doped HAp in distilled water. The dissolved HAp were mounted on agar surface. The whole assemble was brooded for

24h at 37 °C. The zone of growth inhibition was calculated using a ruler.

Samples code	$n(H_3PO_4)$ mmol	$n(CaOH_2)$ mmol	$n(CuO)$ mmol	$n(MgO)$ mmol	Chemical formula
HA-1	60	100	0	0	$Ca_{10}(PO_4)_6(OH)_2$
HA-2	60	90	5.0	5.0	$(Cu_{0.5},Mg_{0.5})Ca_9(PO4)_6(OH)_2$
HA-3	60	90	2.5	7.5	$(Cu_{0.25},Mg_{0.75})Ca_9(PO4)_6(OH)_2$
HA-4	60	90	7.5	2.5	$(Cu_{0.75},Mg_{0.25})Ca_9(PO4)_6(OH)_2$

Table 1. Amounts of reactants needed for preparation of HAp and co-doped HAp.

2.2.4.2 Cytotoxicity investigation

The American Type Culture Collection provided the MC3T3-E1 osteoblast cell line (ATCC, Manassas, VA, USA). The cells were planted at a density of 5000 cells per well in 96-well plates and prior to being used, it was cultured for 24 hours. The cells were rinsed in PBS (phosphate Buffered Saline, pH 7.4) before being cultured in fresh media for 72 hours with different sample concentrations (1000, 750, 500, 250, 125, 0 g/ml). The 3-(4,5dimethylthiazol-2-yl)-2,5-diphenyltetrazolium bromide (MTT) dye reduction assay was used to measure cell viability. MTT was used to test the cytotoxic effect of the specimens at various concentrations. MTT (0.5 mg/mL in PBS) was applied to each well after 72 hours of incubation (37°C, 5% CO2 in a humid environment). The dish was then incubated at 37°C for another 4 hours. The formazan was dissolved in 100 μl DMSO with moderate vibrating at 37°C and the absorbance calculated with an ELISA reader at 570nm.
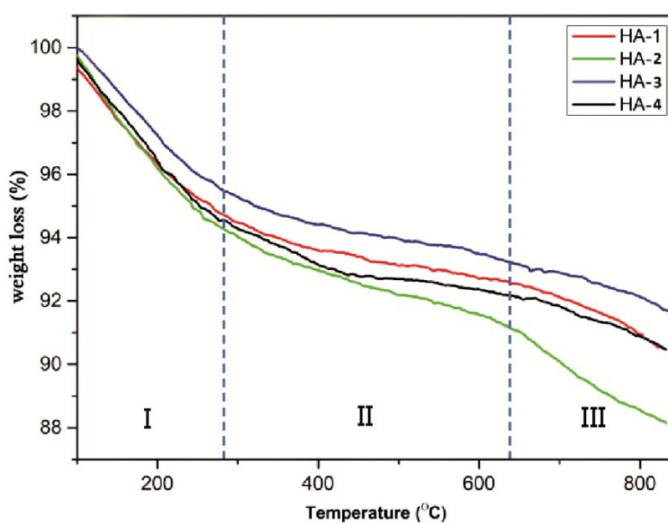
The average of three distinct experiments was used to compute the results.

3. Results and discussion

3.1 Thermal analysis

From the TG carve as demonstrated in Fig.1, the mass loss during heating could be separated into three different steps. First, the weight loss at 200°C which is corresponding to remove the physical adsorbed water. Next, the decomposition of HPO_4^{-2} occurs between 200°C and 65 °C according to the reaction $2HPO_4^{2-} \rightarrow P_2O_7^{4-} + H_2O$ [19]. The evaporated water at this stage represents the intermolecular water. Increasing the temperature above 650°C may lead to react $P_2O_7^{4-}$ and OH^- ion may well have reacted to form PO_4^{3-} and H_2O, according to the reaction $P_2O_7^{4-} + 2OH^- \rightarrow 2 PO_4^{3-} + H_2O$ as reported by Lee et al. and Mardziah et al [20, 21]. The total mass loss of the samples HA-1, HA-3 and HA-4 is about 10% while that of HA-2 is about 12%. The difference in weight loss among the prepared HAp counts on the crystillinity and the stoichiometric ratio [19].

Fig. 1.The relation between weight loss and temperature for undoped and co-doped HAp
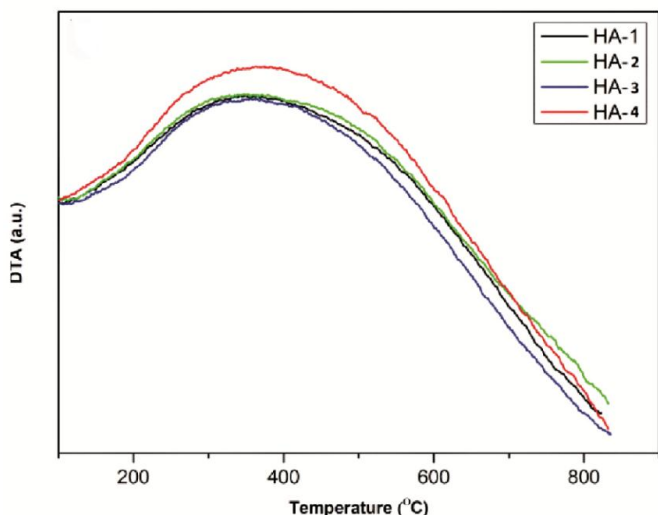

_____

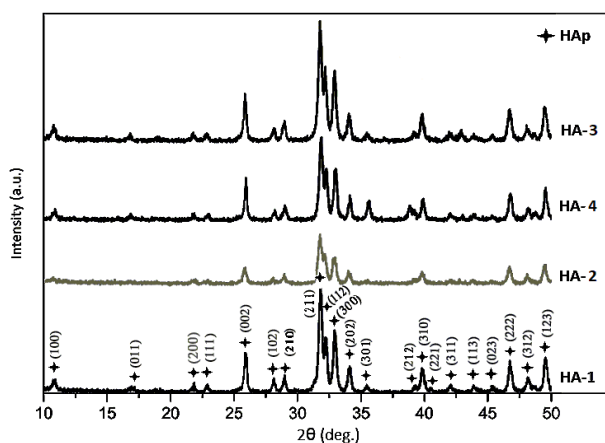Fig. 2. The DTA carves for undoped and co-doped HAp

Fig. 3 : X- ray diffraction patterns of the as-prepared HA and co-doped HA

Suitable temperature for post heat treatment was determined from DTA curves of the prepared HAp as shown in Fig.2. It shows that all curves appear one broad endothermic peak starts a round 200°C and ends at 800°C.

Table 2: Unit cell dimensions and crystallinity of the undoped-HAp and (Cu, Mg) doped HAp

This peak may refer to nonstoichiometric decomposition reactions that involve losing of interstitial water and correcting the stoichiometric ratio of HAp; in addition to enhance structural order of apatite crystallites [22].

3.2 Structural characteristics

The results of X-ray diffraction are illustrated in Fig. 3. It is clear that the yield compound has a pure hexagonal apatite phase without secondary phases (pattern AH-1). The co-doped hydroxyapatites did not show other calcium phosphates (as secondary phases) nor oxides of the dopants
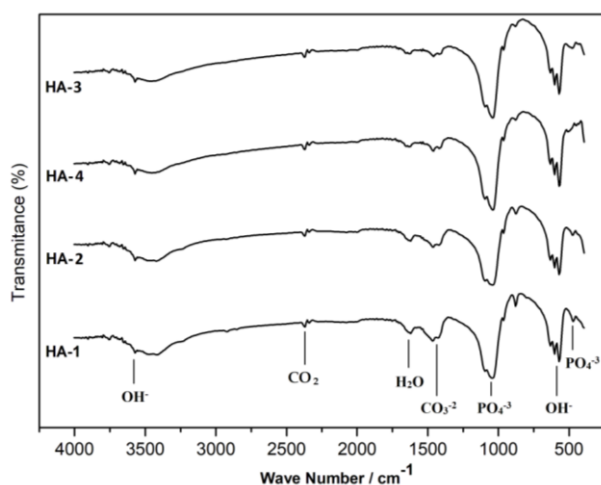
Patterns (HA-2, HA-3, and HA-4) illustrate that the added Cu^{2+} and Mg^{2+} into HA have dissolved well into the apatite crystals where no traces of those ions phases have appeared. The data in Table 2 were measured from the XRD patterns using the origin program. It exhibits that the cell dimensions as well as the crystallinity of the undoped and co-doped hydroxyapatite crystals. The crystal dimensions (a plus b) of undoped HA are about 9.4348 Å, while it is 6.8847 Å for c as showed in Table 2. They are comparable to those of synthesized HA [8, 15].

Introducing new divalent ions (Cu and Mg) into HAp lattice has changed the crystal dimensions as a results of variation in the ions radii among Ca^{2+}, Mg^{2+} and Cu^{2+} (114 pm, 86 pm, 87 pm, respectively). Single substitution of ions were exempted in this work because it has intensively covered in other literature [23, 24, 17]; and the study was focused on the double ions substitution. As illustrated in Table 2 that increasing the substituted mole ratio of copper and decreasing that of magnesium decreases the HA crystal (a, b) dimensions. (c) dimension has slightly changed where no remarkable trend has noticed along with the additions. Vojislav et al. reported that (a, b) lattice dimensions decreased with increasing doped fraction of Cu^{2+} alone. A possible reason for this alteration was as a result of ionic radii differences [15]. The hexagonal unit cell volume also contracts when HAp is doped with Mg^{2+} ions [8].

Composition	a, b (Å)	C (Å)	Volume (Å³)	X_c, (%)
$Ca_{10}(PO_4)_6(OH)_2$	9.4348	6.8847	530.74	81.5
$(Cu_{0.5},Mg_{0.5})Ca_9(PO4)_6(OH)_2$	9.3723	6.8911	524.22	82.2
$(Cu_{0.25},Mg_{0.75})Ca_9(PO4)_6(OH)_2$	9.4277	6.8649	528.42	75
$(Cu_{0.75},Mg_{0.25})Ca_9(PO4)_6(OH)_2$	9.3448	6.8780	520.16	79.3

In fact, adding equal mole ratio of 0.5 of each element has not made that change in a- and b-dimensions, where they were 9.4348 Å before and 9.4277 Å after. However, c dimension was a bit decreased from 6.8847 Å to 6.8649 Å. The degree of crystallinity (X_c) (degree of structure order) was calculated for undoped and doped HAp as shown in Table 2. The added ions in the structure of hydroxyapatite not just have an effect to the dimensions of the lattice but have led to decrease the crystallinity of HA. Sharp peaks in Fig. 3 confirms that they are highly crystallized. The crystallinity of as-prepared HA is about 81.5%. The same degree of order can be seen with the chemical $(Cu_{0.25}, Mg_{0.75})Ca_9(PO_4)_6(OH)_2$. Increasing of Cu content and lowing Mg content led to lowering the crystallinity below 80%, where the minimum crystallinity was recorded to HA-2 of about 75%. This may cause high distortion in the ions configuration in the lattice of HAp. It is known that the crystallinity of the hydroxyapatite counts on the preparation method. Precipitation temperature, pH and aging time are crucial in the wet chemical precipitation method [15].

Lazi´c et al. hydroxyapatite can show high crystallinity at a precipitation temperature range of 22°C – 95°C and at a maximum maturing time of 20h [19]. Fig.4 shows FTIR spectra of the functional groups $(PO_4^{3-}$ and $OH^-)$ in the HAP lattice. The spectra of sample HA-1 reveals the characteristic bands of absorbed water (hydroxyl group) at around 570 cm^{-1} and at 3471-3417 cm^{-1}. The band at 1041cm^{-1} and 462 cm^{-1} associate with the stretching modes of the PO_4^{-3} related to HA.

Fig. 4. Functional groups of as-precipitated hydroxyapatite with different compositions

The band at 1620cm^{-1} is assigned for the stretching modes of H_2O bond. The bands attributed to CO_3^- was observed in (1427, and 1458 cm^{-1}), and the bands at 2468 cm^{-1} attributed to CO_2 according to Álvarez et al [16]. These bands are found in all samples but they have different band intensities with a slight shifting

3.3 Microstructural observations

The shape of HAp particles are depicted in the TEM micrographs of the undoped and the co-doped HAp see Fig. 5. After a 2-hour heat treatment at 850°C, all of the samples were investigated. Two compositions were chosen to be investigated depending on the Antibacterial effect which were pure HAp and $(Cu_{0.25}, Mg_{0.75})Ca_9(PO4)_6(OH)_2$. Fig. 5 reveals that the particle size is within the nano range (<100 nm) and they became longer in c-direction in comparison to the undoped HAp. The TEM micrographs are support the X-ray diffraction results that have showed increasing c- and decreasing a- and b-directions of HAp crystals after substituting Cu^{2+} by Mg^{2+} and Ca^{2+}.

3.4 Antimicrobial activity

The findings of antibacterial investigation showed that the antimicrobial activity has varied according to the chemical modification. Fig. 6 exhibits different responses of the synthesized HA. Undoped HA (HA-1) and co-doped HA (HA-2) didn't show any effect against either Gram(+) as S.aureus or Gram(-) as E.coli bacteria. This means that these compositions cannot fight the effect of the bacterial media. On the other side, the composition denoted as HA-3 and HA-4 exhibited shows remarkable effect on the E.coli, while on the S. arueus the *behaviour* was slightly lower. This can be inferred from the *grey* ring diameter in Fig. 6 It is clear that specimen HA-4 shows the biggest diameter (30 mm). The gray zone diameter relay on the mole ratio of Cu^{2+} and Mg^{2+} in HAp.

The results also indicates that Mg2+ has low influence on the inhibition of bacteria activity. It is inferred that addition of Cu2+ is more valuable for the co-doped HAp in fighting infection of implants or for other clinical usages. Magnesium, on the other hand, showed little contribution to inhabit the bacteria activity as seen in the gray zone diameter. One possible reason is that Cu+2 ions engage with bacterial cell membranes, altering their structure, eventually, death of cell [26]. Fig. 6 shows different responses for HA in E.coli and in S.aureus bacteria. This can belong to the S. aureus membrane structure of Gram+ which makes it less vulnerable to all metal-doped HA than E. coli bacteria [15].
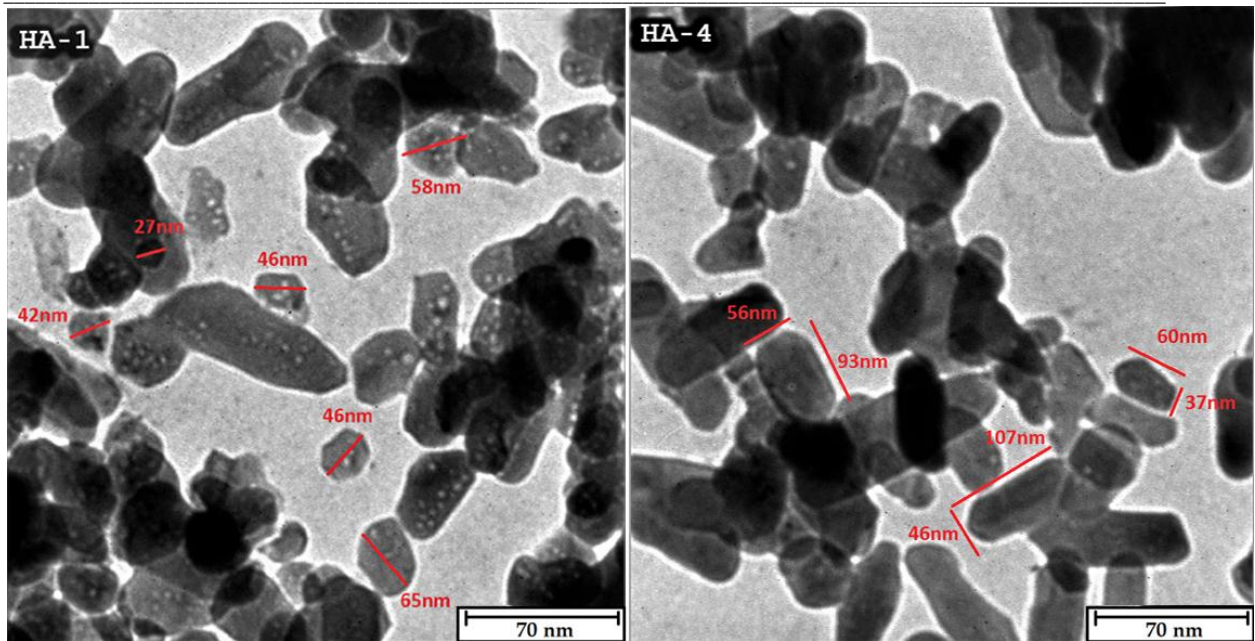
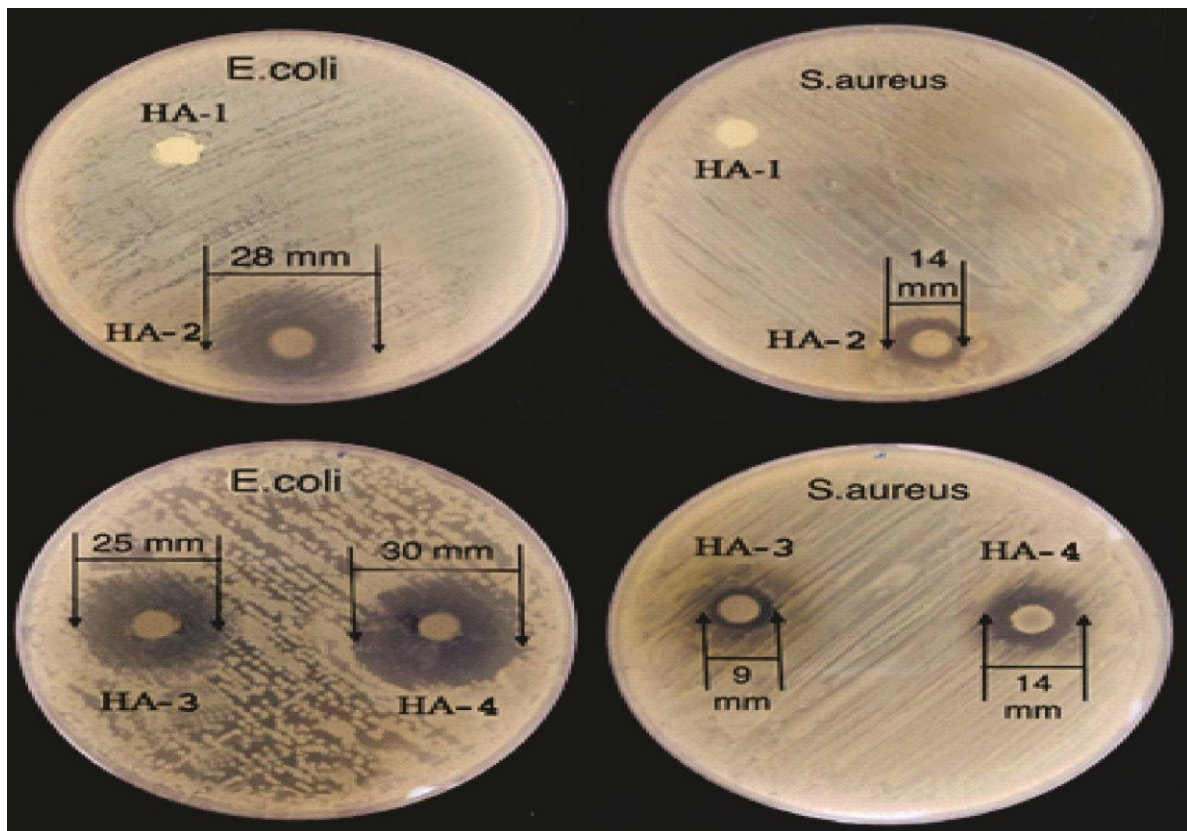Fig. 5 :TEM micrograph of the hydroxyapatite powders, HA-4 (Co-doped HA), HA-1 (undoped HA)

Fig. 6 . Antibacterial response of the synthesized HAp against E. coli and S. aureus bacteria

_____

3. 3.5 Cytotoxicity investigation

The MTT assay was used to determine the viability of osteoblast cells as shown in Fig. 7. It reveals that the cells viability are reversely related to the concentration of dissolved HAp where it is about 76.8% at 125 mg/ml. Fig. 7 exhibits that HAp alone showed lower performance in comparison to co-doped HAp. No matter how the concentration of dissolved HAp is($Mg_{0.75}$, $Cu_{0.25}$) it appears no toxic effect , This can be inferred by the abundance of survival cells. In fact, Magnesium has a high biocompatibility with living cells and helps to mend bones by encouraging osteoblast proliferation during the initial stages of osteogenesis according to T.Tite et. al [27]. It can enhance osteoblast growth subsequently bone regeneration by accelerating mineral metabolism. It is well known that copper is a toxic element to the live tissues .However, decreasing the concentration of copper can well do as antibacterial agent. HA-4 exhibits the lowest live cells all the intended concentrations which indicates a toxic effect which contains 0.75 % Cu^{2+}. Images of the live and healthy cells after 3 days of cultural periods for different HAp concentrations.

It has been noticed that the choice of dopant ions influences the cells environment . Fig. 8 supports the results of MTT assay, where the density of live cells vary according to the amount of additive element added and to the concentration of the dissolved HAp. In comparison to HA-1 and HA-4, the presence of Mg2+ can improve osteoblast development and encourage bone regeneration by accelerating mineral metabolism and increasing catalytic events during the bone remodeling process, This can be seen by increasing the number of the blue spots in Fig. 8.

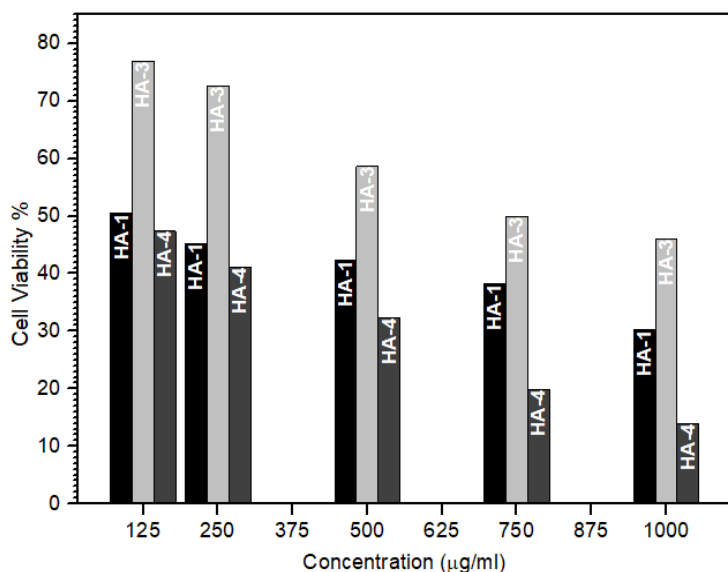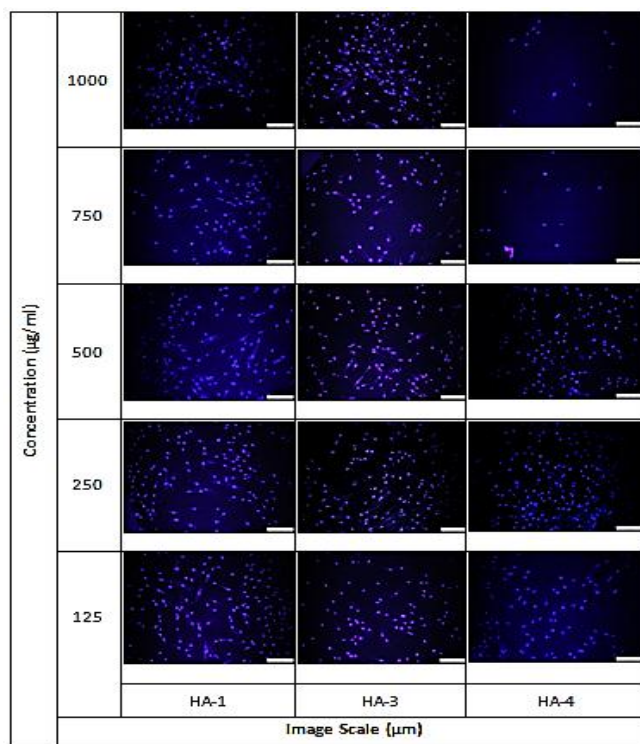Fig. 7. Cell viability from MTT assay for different concentrations of pure and co-doped HAp powders

Fig. 8. Microscopic pictures of osteoblast cells at various concentrations of undoped and co-doped HAp

Controversially, increasing the concentration of copper in the HAp lower the number of osteoblasts where the cell underwent lysis.

So the cytotoxicity assay revealed that osteoblast cell was killed when high concentration of Cu^{2+} exists in their environment [16]. In fact, presence of copper makes confluence and proliferation of live cells at minimum as inferred from Fig.8.

4. Conclusions

HAp and co-doped HAp nanoparticles with a mole ratio (Cu+Mg+Ca)/P of 1.67 were successfully synthesized using the wet chemical precipitation method. It can be inferred that dopants (Cu^{2+} and Mg^{2+}) well entered in the structure of HAp. As a result they influence the shape of yield crystals where they elongated in c-direction and diminished a bit in a- and b-directions according to the ions radii. The particle size after calcination was in the range of 50 - 100 nm. The behaviour of co-doped HAp varied as the amounts of additive elements varied. High copper and lower magnesium HAp worked very good against bacteria. While high magnesium and lower copper has a greater positive effect on cell viability compared to Cu^{2+} which enhanced osteoblasts growth and it showed the minimum cytotoxicity among the prepared HAp.

_____

8. References

[1] S. Dorozhkin , Calcium Orthophosphates Applications in Nature, Biology, and Medicine, Pan Stanford Publishing CRC Press, U.S, 2012.

[2] J. T U , M.Senthilkumar , Preparation And Characterization Of Pure And Silver Nitrate Doped Nano Hydroxyapatite For Biomedical Applications, *International Journal of Technical Research and Applications*. 37 (2016) 32-37.

[3] I. Mobasherpour , M. Soulati Heshajin , A. Kazemzadeh , M. Zakeri , Synthesis Of Nanocrystalline Hydroxyapatite By Using Precipitation Method , *Journal of Alloys and Compounds*. 430 (2007) 330–333. Doi: /10.1016/j.jallcom.2006.05.018

[4] M. Mucalo ,Hydroxyapatite (HAp) for Biomedical Applications , Woodhead Publishing, Elsevier ,UK ,2015.

[5] M. Riaz ,R. Zia ,A. Ijaz ,T. Hussain ,M. Mohsin , A. Malik , Synthesis of monophasic Ag doped Hydroxyapatite and evaluation of Antibacterial activity , *Materials Science & Engineering C*., 90 (2018)   308   313   . doi:10.1016/j.jallcom.2006.05.018.

[6] O. Kaygili , S. Keser , Sol–Gel Synthesis and Characterization of Sr/Mg, Mg/Zn and Sr/Zn Co-Doped Hydroxyapatites, *Materials. Lettes*, 141 (2015)   161–164. doi:10.1016/j.jallcom.2006.05.018.

[7] A. Rajendran, S. Balakrishnan, R. Kulandaivelu, S. Narayanan, S. Nellaiappan, Multi-element substituted hydroxyapatites: synthesis, structural characteristics and evaluation of their bioactivity, Cell Viability, and antibacterial activity, *Journal of Sol-Gel Science and Technology*.10 (2018) 561–   756. https://doi.org/10.1007/s10971-018-4634-x.

[8] Z. Evis, T. J. Webster, Nanosize Hydroxyapatite: Doping with various ions, *Advances in Applied Ceramics*., 110 (2011) 5 – 311. doi. 10.1179/1743676110Y.0000000005.

[9] S. Bodhak, S. Bose, A. Bandyopadhyay, Influence of MgO, SrO, and ZnO Dopants on Electro-Thermal Polarization Behavior and In Vitro Biological Properties of Hydroxyapatite Ceramics, *Journal of the American Ceramic Society. Soc*. 94 (2011) 1281–1288. doi: 10.1111/j.1551-2916.2010.04228.x.

[10] S. Kannan, F. Goetz-Neunhoeffer, J. Neubauer, J. M. F. Ferreira, Ionic Substitutions In Biphasic Hydroxyapatite and B-Tricalcium Phosphate Mixtures: Structural Analysis By Rietveld Refinement, *Journal of the American Ceramic Society*. 91 (2008) 1–12. doi: 10.1111/j.1551-2916.2007.02117.x.

[11] J. Kolmas, E. Groszyk D. Kwiatkowska, Substituted Hydroxyapatites With Antibacterial Properties, *Bio Med Research International*., (2014)   Article   ID   178123. http://dx.doi.org/10.1155/2014/178123.

[12] S.A. Abidi , Q.Murtaza, Synthesis and Characterization of Nanohydroxyapatite Powder using Wet Chemical Precipitation Reaction , *U.P.B. Sci. Bull.*, 75 (2013) 1454-2331.

[13] S. Ramesh, S. Adzila , C.K.L. Jeffrey, C.Y. Tan ,J. Purbolaksono, A.M. Noor, M.A. Hassan, I. Sopyan , W.D. Teng, Properties of Hydroxyapatite Synthesize by Wet Chemical Method , *Journal of Ceramic Processing Research*., 14 (2013) 448–452.

[14] D. S. Gomes, A. M. C. Santos, G. A. Neves , R. R. Menezes , A Brief Review on Hydroxyapatite Production and use In Biomedicine, *Cerâmica*, 65 (2019) 282-302. http://dx.doi.org/10.1590/0366-69132019653742706.

[15] V. Stanic ,S. Dimitrijevic, J.A. Stankovic ,M. Mitric , B.Jokicb ,I. B. Plecas S. Raicevic, Synthesis, Characterization and Antimicrobial Activity of Copper and Zinc-Doped Hydroxyapatite Nanopowders , *Applied Surface Science*. 256 (2010) 6083–6089. doi:10.1016/j.apsusc.2010.03.124.

[16] Y. Li, J. Ho , C.P. Ooi , Antibacterial Efficacy and Cytotoxicity Studies of Copper (II) And Titanium (IV) Substituted Hydroxyapatite Nanoparticles , *Materials Science and Engineering* . 30 (2010) 1137–1144. http://dx.doi.org/10.1016/j.msec.2010.06.011.

5. [17] H. Alioui ,O. Bouras , J.C. Bollinger , Toward an efficient antibacterial agent: Zn- and Mg-doped hydroxyapatite nanopowders , *Journal of Environmental Science and Health*.54 (2019) 315–327. https://doi.org/10.1080/10934529.2018.1550292.

[18] D. Gopi, S. Ramya, D. Rajeswari, P. Karthikeyan , L. Kavitha, Strontium, Cerium Co-Substituted Hydroxyapatite Nanoparticles: Synthesis, Characterization, Antibacterial Activity Towards Prokaryoticstrains and in Vitro Studies, *Colloids and Surfaces A: Physicochemical and*

_____

Engineering Aspects .451, (2014), 172–180. http://dx.doi.org/10.1016/j.colsurfa.2014.03.035.

[19] S. Lazic, S.Zec, N.Miljevic, S.Milonjic, The Effect of Temperature on The Properties of Hydroxyapatite Precipitated From Calcium Hydroxide And Phosphoric Acid .*Thermochimica. Acta*. 374 (2001) 13 –22.

[20] I.H. Lee, J.A. Lee, J.H. Lee, Y.W. Heo, J.J. Kim , Effects of PH and Reaction Temperature on Hydroxyapatite Powders Synthesized by Precipitation, *Journal of the Korean Ceramic Society*. 57 (2020) 56–64. https://doi.org/10.1007/s43207-019-00004-0.

[21] C.M. Mardziah, I. Sopyan, S. Ramesh, Strontium-Doped Hydroxyapatite Nanopowder Via Sol-Gel Method: Effect of Strontium Concentration and Calcination Temperature On Phase Behavior, *Trends Biomater. Artif. Organs*, 23 (2009) 105–113. https://www.researchgate.net/publication/249011460.

[22] L. Stipniece, K. Salma-Ancane, N. Borodajenko, M. Sokolova, D. Jakovlevs , L. Berzina-Cimdina, Characterization of Mg-Substituted Hydroxyapatite Synthesized by Wet Chemical Method. *CERAMICS INTERNATIONAL*. 40 (2014) 3261–3267. http://dx.doi.org/10.1016/j.ceramint.2013.09.110.

[23] C.P.Álvarez, J.S.C.Sarmiento, S.C.Freitas, Claudia García, Solvothermal Synthesis of Magnesium Oxide-Substituted Hydroxyapatite Nanoparticles as Antibacterial Nanomaterial for Biomedical Applications, *Defect and Diffusion Forum.* 381(2017) 8-14. https://doi.org/10.4028/www.scientific.net/DDF.381.8.

[24] D. Predoi, S.L. Iconaru, M.V. Predoi, G.E. Stan, N. Buton, Synthesis, Characterization, and Antimicrobial Activity of Magnesium-Doped Hydroxyapatite Suspensions, *Nanomaterials.* (2019). doi: 10.3390/nano9091295.

[25] E. Landi, A. Tampieri, G. Celotti, S. Sprio, Densification behavior and mechanisms of synthetic hydroxyapatites, *Journal of the European Ceramic Society.*20 (2000) 2377–2387.doi. PII: S0955-2219(00)00154-0.

[26] W.L. Du, Y.L. Xu, Z.R. Xu, C.L. Fan, Preparation, Characterization and Antibacterial Properties Against E. Coli K88 of Chitosan Nanoparticle Loaded Copper Ions, *Nanotechnology*. 19 (2008). https://ur.booksc.eu/book/23096804/1b18a3.

[27] T.Tite , A.C. Popa and G.E. Stan , Cationic Substitutions in Hydroxyapatite: Current Status of the Derived Biofunctional Effects and Their In Vitro Interrogation Methods , *materials* , 11 (2018) 2081. http://dx.doi.org/10.3390/ma11112081.

_____